

Classification of atomic states by geometrical and quantum-mechanical symmetries

M. D. Poulsen and L. B. Madsen

Department of Physics and Astronomy, University of Aarhus, 8000 Århus C, Denmark

(Received 23 June 2005; published 10 October 2005)

The eigenstates of nonrelativistic two-, three-, four-, and six-valence-electron atoms are classified according to their transformation properties under symmetry operations. In energy-favorable geometrical arrangements of the electrons, the spatial distribution of the wave function is constrained by the demand of invariance under rotation, inversion and permutation of particles. For a given term, the symmetry constraints may leave the energy-favorable arrangement accessible or inaccessible. In the latter case the term is not expected to belong to the low-energy part of the spectrum. Contrary, in the former case with no symmetry-induced inherent nodal surface in the multidimensional coordinate space of the multielectron wave function, the term is expected to belong to the low-energy part of the spectrum. The symmetry-based classification is confirmed by recent calculations.

DOI: [10.1103/PhysRevA.72.042501](https://doi.org/10.1103/PhysRevA.72.042501)

PACS number(s): 31.10.+z, 31.25.-v

I. INTRODUCTION

Geometrical images and symmetries of the motion of electrons around the positive nucleus were essential elements in the early attempts made to understand the constitution of atoms (see, e.g., Refs. [1,2]). The development of “modern” quantum mechanics [3,4] and very effective mean-field theories [5,6] in combination with Racah algebra, however, clearly defined mathematically and computationally the problem of determining atomic structure and it is fair to say that geometrical considerations to a large extent were rendered superfluous. This picture changed to some extent with the work on multiple-particle breakup close to threshold [7]. Here the line-configuration [Fig. 1(a)] was essential for the analysis of the two-electron escape [7]. Similarly, the equilateral triangle configuration [Fig. 1(b)] and the regular tetrahedron [Fig. 1(c)] were used in the analysis of the escape of three [8] and four electrons [9,10] from the nucleus. More recently, a unified approach for the near-threshold multiple-particle breakup was developed in a series of papers [11–13]. Also, below threshold, geometrical images of the correlated electron dynamics have been helpful in the characterization of doubly and multiply excited states. For doubly excited states such physical pictures helped in developing the present understanding of the correlated motion of the two excited electrons in terms of breathing and asymmetric stretch modes [14,15]. Also for three-electron atoms, pictures of the relative motion of three excited electrons led to a classification in terms of different modes [see Ref. [16] and references therein] and, in particular, the equilateral triangle configuration was used in the development of the so-called symmetric rotor model [17]. Several models for triply excited states were recently reviewed in Ref. [18]. For four electrons the regular tetrahedron [Fig. 1(c)] was used to derive a classification scheme for quadruply excited states [19–21]. The original idea promoted in these works was to classify the multiply excited states by means of inherent nodal surfaces. Recently, the symmetric rotor model was extended to the case of four excited electrons [22].

Classification schemes based on geometrical and quantum-mechanical symmetry were considered previously

[19–21,23–26]. In this work we consider the method outlined in these works, describe how to obtain such a classification, and apply the approach to two-, three-, four-, and six-valence-electron systems. The method is particularly useful for multiply excited states whose classification is typically difficult to address using standard computational techniques.

The paper is organized as follows. In Sec. II, geometrical symmetry operations are considered. In Sec. III, the constraints set by quantum mechanical symmetries are discussed, and a linear set of classification equations is derived. In Sec. IV, this set is investigated and a general compact notation is introduced. In Sec. V, the results are presented, Sec. VI con-

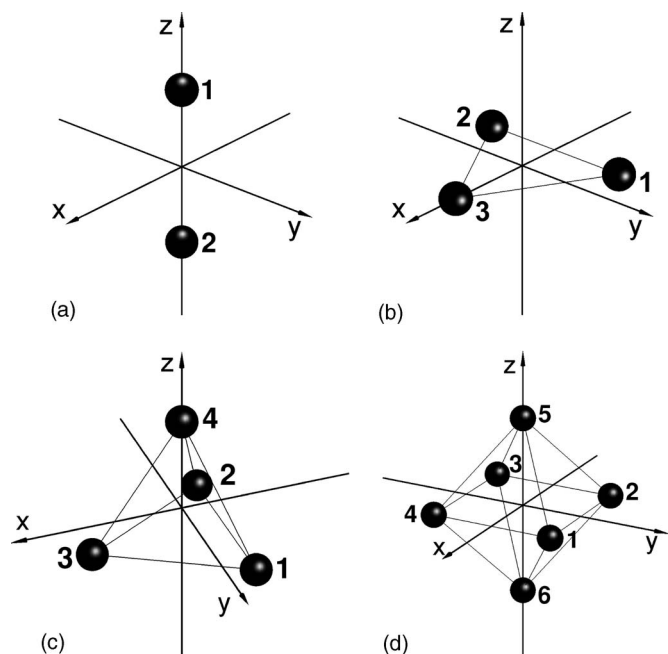


FIG. 1. Energy-favorable geometrical configurations for (a) two-, (b) three-, (c) four- and (d) six-valence-electron atoms. The nuclei are imagined to be in the respective origins. The orientations of the coordinate systems are chosen in order to visualize as clearly as possible the three-dimensional structures.

cludes, and Appendix A presents elements of group theory as required by the present work.

II. GEOMETRICAL SYMMETRIES

For a multielectron atomic system the energetically most favorable geometric configuration minimizes the electron-electron repulsion. For two-electron systems this geometry corresponds to the case where the two electrons are diametrically opposite with respect to the nucleus; see Fig. 1(a) (line configuration). For the three-electron system, the energy is minimized when the electrons form an equilateral triangle (ET) with the in-plane nucleus in the center [Fig. 1(b)]. For systems with four and six electrons, the most favorable configurations are obtained by placing the electrons in the vertices of a regular tetrahedron (RTH) or a regular octahedron (ROH), respectively [Figs. 1(c) and 1(d)]. Note that the symmetry of the five-electron system is low compared to the systems in Fig. 1, since no regular polyhedron in \mathbb{R}^3 minimizes the potential energy of the system.

The body-fixed frames for the systems shown in Figs. 1(a)–1(d) are inspired by molecular theory. The rotational state of a molecule is determined by the quantum numbers L , M , and M_I which specify the total angular momentum and its projection on the space-fixed and the body-fixed quantization (z) axis, respectively. The quantum number M_I is conserved only if the moments of inertia with respect to the body-fixed x and y axes are equal. Both the RTH and ROH configurations are spherical tops and, consequently, we may choose the body-fixed frames by convenience.

A. Two-electron systems

A combination of any two of the following operations leaves the two-electron system [Fig. 1(a)] unchanged:

$$\mathbf{I}, \mathbf{P}_{12}, \mathbf{R}_\pi^y, \mathbf{R}_\pi^x, \quad (1)$$

where \mathbf{P}_{12} denotes a permutation of the two particles, \mathbf{I} is the operator of space inversion and \mathbf{R}_θ^k is the operator of rotation about the k axis by an angle θ . The operation \mathbf{R}_π^x is equivalent to the three successive rotations $\mathbf{R}_{-\pi/2}^y \mathbf{R}_\pi^z \mathbf{R}_{\pi/2}^y$, which is a more convenient expression since the Wigner functions of rotations are determined with respect to fixed y and z axes [27]. As a result, the line configuration is invariant to the following operations:

$$\mathbf{O}_a = \mathbf{I} \mathbf{P}_{12}, \quad (2)$$

$$\mathbf{O}_b = \mathbf{I} \mathbf{R}_\pi^y, \quad (3)$$

$$\mathbf{O}_c = \mathbf{I} \mathbf{R}_{-\pi/2}^y \mathbf{R}_\pi^z \mathbf{R}_{\pi/2}^y. \quad (4)$$

B. Three-electron systems

The ET configuration of Fig. 1(b) is invariant under the following three types of operations:

$$\mathbf{O}_d = \mathbf{R}_\pi^z \mathbf{I}, \quad (5)$$

$$\mathbf{O}_e = \mathbf{P}_{132} \mathbf{R}_{2\pi/3}^z, \quad (6)$$

$$\mathbf{O}_f = \mathbf{P}_{12} \mathbf{R}_\pi^y \mathbf{I}, \quad (7)$$

where \mathbf{P}_{132} denotes the cyclic permutation $1 \rightarrow 3 \rightarrow 2 \rightarrow 1$.

C. Four-electron systems

The RTH configuration of Fig. 1(c) is invariant to the operations

$$\mathbf{O}_g = \mathbf{P}_{132} \mathbf{R}_{2\pi/3}^z, \quad (8)$$

$$\mathbf{O}_h = \mathbf{P}_{12} \mathbf{R}_\pi^y \mathbf{I}, \quad (9)$$

$$\mathbf{O}_i = \mathbf{P}_{124} \mathbf{R}_\Phi^y \mathbf{R}_{2\pi/3}^z \mathbf{R}_{-\Phi}^y, \quad (10)$$

with $\Phi = 2 \arccos(1/\sqrt{3}) = 109.5^\circ$ being the interelectronic angle as seen from the nucleus.

D. Six-electron systems

Finally, the ROH configuration of Fig. 1(d) is invariant to the operations

$$\mathbf{O}_j = \mathbf{P}_{13} \mathbf{P}_{24} \mathbf{P}_{56} \mathbf{I}, \quad (11)$$

$$\mathbf{O}_k = \mathbf{P}_{1234} \mathbf{R}_{-\pi/2}^z, \quad (12)$$

$$\mathbf{O}_l = \mathbf{P}_{12} \mathbf{P}_{34} \mathbf{P}_{56} \mathbf{R}_\pi^y, \quad (13)$$

$$\mathbf{O}_m = \mathbf{P}_{253} \mathbf{P}_{146} \mathbf{R}_{-\Theta}^y \mathbf{R}_{2\pi/3}^z \mathbf{R}_\Theta^y, \quad (14)$$

where $\Theta = \frac{1}{2}\Phi = 54.74^\circ$. As an example, the effect of the operator \mathbf{O}_m is demonstrated in Fig. 2.

III. QUANTUM-MECHANICAL SYMMETRIES AND USE OF GROUP THEORY

The classification of atomic states relies on the fact that the total electronic angular momentum, spin, and parity commute with the nonrelativistic Hamiltonian of the Coulomb system. Here, we assume the validity of the LS -coupling scheme and describe the atomic states by a wave function, $|\Psi^{LM\pi, SM_s}\rangle$, where L is the total angular momentum of the state, M the magnetic quantum number, π the parity, S the total spin, and M_s its projection.

It is, in general, possible to expand an antisymmetrized eigenstate of identical fermions in a sum of products of spatial functions, $F_{Mi}^{L\pi S}$, and spin functions $\chi_{M_s i}^S$,

$$|\Psi^{LM\pi, SM_s}\rangle = \sum_i F_{Mi}^{L\pi S} \chi_{M_s i}^S, \quad (15)$$

where the summation is over all possible couplings of intermediate spin. In writing up this expression, we imply that the totally antisymmetric wave function is constructed as a sum of spatial functions belonging to specific Young tableaux multiplied with spin functions belonging to conjugate tableaux (see Appendix A). Throughout we use the standard irreducible basis of the permutation group, referred to as the

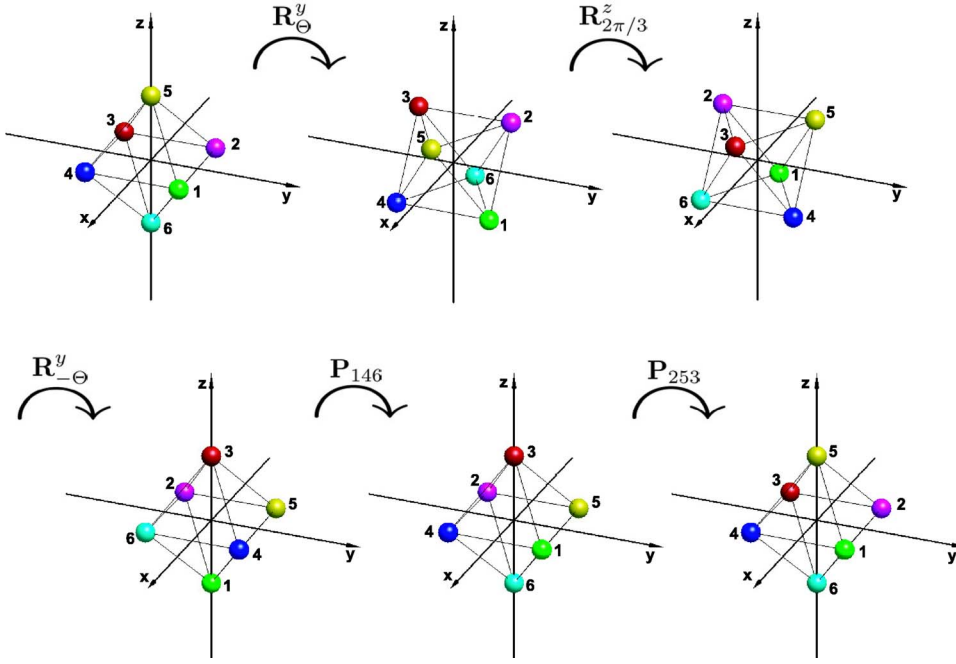


FIG. 2. (Color online) The effect of the operator, $\mathbf{O}_m = \mathbf{P}_{253}\mathbf{P}_{146}\mathbf{R}_{-\Theta}^y\mathbf{R}_{2\pi/3}^z\mathbf{R}_{\Theta}^y$ with $\Theta = 54.74^\circ$, on six electrons placed at the vertices of a regular octahedron (ROH).

Young-Yamanouchi basis. In Eq. (15), the value of the spin S determines the representation and therefore the Young tableaux. Accordingly, when we use the symbol $F_{Mi}^{L\pi S}$, it is understood that this spatial wave function has a particular associated Young tableau (the conjugate of the tableau of the spin wave function). This is used in our evaluation of the matrix elements of the permutation operator below.

For a given intermediate spin coupling, the examination of the transformation properties of the spatial part is straightforward. Only the relative positions of the electrons and the nucleus are of interest, the overall rotation with respect to a fixed laboratory frame is unimportant. The spatial wave functions are, therefore, expanded through rotations as

$$F_{Mi}^{L\pi S} = \sum_{M_i} D_{M_i M}^L(-\omega) F_{M_i, \omega}^{L\pi S}, \quad (16)$$

where $F_{M_i, \omega}^{L\pi S}$ refers to a rotated body-fixed frame determined by the Euler angles $\omega = (\alpha, \beta, \gamma)$ describing rotations around fixed z , y , and z axes, respectively. The Wigner functions $D_{M_i M}^L(-\omega)$ are the matrix elements of the rotation matrix $\mathbf{R}(-\omega)$ [27].

The fact that the energy-favorable configurations are invariant to the symmetry operations in Eqs. (2)–(14) implies that the values of the spatial functions, $F_{M_i, \omega}^{L\pi S}$, at these configurations have to be invariant to the symmetry operations. Consequently, the wave function is constrained by the condition

$$F_{M_i, \omega}^{L\pi S}(\text{conf}) = [\mathbf{O}_\rho F_{M_i, \omega}^{L\pi S}]_{\text{conf}}, \quad (17)$$

where ‘‘conf’’ denotes the line-, ET, RTH, or ROH configuration depending on the system, and ρ is a symmetry operation of the system in question. In the following, the subscript ω referring to the Euler angles is left out. As an example, Eq. (17) for the six-electron system reads

$$F_{M_i}^{L\pi S}(\text{ROH}) = [\mathbf{O}_\rho F_{M_i}^{L\pi S}]_{\text{ROH}}, \quad \rho \in \{j, k, l, m\} \quad (18)$$

with \mathbf{O}_ρ given in Eqs. (11)–(14).

For each of the systems in Fig. 1, Eq. (17) yields a set of homogeneous linear equations for the coefficients, $F_{M_i}^{L\pi S}$, at the respective energy-favorable configurations. This set only depends on L , π , and S , and the question is whether non-trivial solutions exist or not. If the set of equations has only the trivial solution, then the term, $^{2S+1}L^\pi$ is inaccessible. In other words, the wave function, $|\Psi^{LM\pi, SM_s}\rangle$, has an inherent nodal surface and the term is not expected to belong to the low-lying part of the energy spectrum. On the other hand, if a nontrivial solution to the set of equations exists, then the term, $^{2S+1}L^\pi$, is accessible. In this sense the present approach gives rise to a classification scheme.

IV. CLASSIFICATION EQUATIONS

The effects of the symmetry operators operating on the functions, $F_{M_i}^{L\pi S}$, are

$$\mathbf{I} F_{M_i}^{L\pi S} = \pi F_{M_i}^{L\pi S}, \quad (19)$$

$$\mathbf{R}_\theta^z F_{M_i}^{L\pi S} = e^{-i\theta M_i} F_{M_i}^{L\pi S}, \quad (20)$$

$$\mathbf{R}_\theta^y F_{M_i}^{L\pi S} = \sum_{M_i'} d_{M_i' M_i}^L(\theta) F_{M_i'}^{L\pi S}, \quad (21)$$

$$\mathbf{P} F_{M_i}^{L\pi S} = \sum_{i'} G_{ii'}^S(\mathbf{P}) F_{M_i'}^{L\pi S} \quad (22)$$

where $d_{M_i' M_i}^L(\beta) = D_{M_i' M_i}^L(0, \beta, 0)$ [27], and $G_{ii'}^S(\mathbf{P}) = \langle F_{M_i'}^{L\pi S} | \mathbf{P} | F_{M_i}^{L\pi S} \rangle$ is a matrix element of the matrix representation in the Young-Yamanouchi basis. In Appendix A it is

TABLE I. Matrix representations $X \in \mathcal{M}_{2L+1}$, $Y \in \mathcal{M}_g$ of the symmetry operations in Eqs. (2)–(14) adjusted to the notation of Eq. (30). The indices jk denote an entrance in the matrix.

	Two electrons	Three electrons	Four electrons	Six electrons
X_{jk}^1	$\pi \delta_{jk}$	$\pi(-1)^{j-L-1} \delta_{jk}$	$e^{-i2\pi/3(j-L-1)} \delta_{jk}$	$\pi \delta_{jk}$
Y_{jk}^1	$G_{jk}^S(\text{P}_{12})$	δ_{jk}	$G_{jk}^S(\text{P}_{132})$	$G_{jk}^S(\text{P}_{13}\text{P}_{24}\text{P}_{56})$
X_{jk}^2	$(-1)^L \delta_{2L+2-j,k}$	$e^{-i2\pi/3(j-L-1)} \delta_{jk}$	$\pi(-1)^{j+1} \delta_{2L+2-j,k}$	$e^{i\pi/2(j-L-1)} \delta_{jk}$
Y_{jk}^2	δ_{jk}	$G_{jk}^S(\text{P}_{132})$	$G_{jk}^S(\text{P}_{12})$	$G_{jk}^S(\text{P}_{1234})$
X_{jk}^3	$\pi(-1)^{j-L-1} \delta_{jk}$	$(-1)^L \delta_{2L+2-j,k}$	$H_{jk}^L(\Phi)$	$(-1)^{j+1} \delta_{2L+2-j,k}$
Y_{jk}^3	δ_{jk}	$G_{jk}^S(\text{P}_{12})$	$G_{jk}^S(\text{P}_{124})$	$G_{jk}^S(\text{P}_{12}\text{P}_{34}\text{P}_{56})$
X_{jk}^4				$H_{jk}^L(\Theta)$
Y_{jk}^4				$G_{jk}^S(\text{P}_{253}\text{P}_{146})$

discussed how to determine the permutation matrices, $G^S(\text{P})$. The dimension of the matrices, $g = \text{size}[G^S(\text{P})]$, corresponds to the number of possible ways to couple the intermediate spins to the total spin S . Hence, the number of unknown variables, $F_{M_i}^{L\pi S}$, for each term, ${}^{2S+1}L^\pi$, is $g \times (2L+1)$ corresponding to g different spin couplings for each value of $|M_i| \leq L$. As an example, Eq. (17) for the six-electron system reads

$$F_{M_i}^{L\pi S}(\text{ROH}) = \pi \sum_{i'} G_{ii'}^S(\text{P}_{13}\text{P}_{24}\text{P}_{56}) F_{M_{i'}}^{L\pi S}(\text{ROH}), \quad (23)$$

$$F_{M_i}^{L\pi S}(\text{ROH}) = e^{i\pi/2M_i} \sum_{i'} G_{ii'}^S(\text{P}_{1234}) F_{M_{i'}}^{L\pi S}(\text{ROH}), \quad (24)$$

$$F_{M_i}^{L\pi S}(\text{ROH}) = (-1)^{L+M_i} \sum_{i'} G_{ii'}^S(\text{P}_{12}\text{P}_{34}\text{P}_{56}) F_{-M_{i'}}^{L\pi S}(\text{ROH}), \quad (25)$$

$$F_{M_i}^{L\pi S}(\text{ROH}) = \sum_{M_{i'}} H_{M_i M_{i'}}^L(\Theta) G_{ii'}^S(\text{P}_{253}\text{P}_{146}) F_{M_{i'}}^{L\pi S}(\text{ROH}), \quad (26)$$

where $G_{ii'}^S(\text{P})$ denote matrix elements of permutation in S_6 and the matrix elements $H_{M_i M_{i'}}^L(\theta)$ are given by

$$\begin{aligned} H_{M_i M_{i'}}^L(\theta) &= \langle LM_i' | \mathbf{R}_{-\theta}^y \mathbf{R}_{2\pi/3}^z \mathbf{R}_{\theta}^y | LM_i \rangle \\ &= \sum_{M_i''} d_{M_i'' M_i'}^L(\theta) d_{M_i'' M_i}^L(\theta) e^{-i2\pi/3 M_i''}. \end{aligned} \quad (27)$$

General solution

To determine whether the linear set of equations obtained from Eq. (17) has a nontrivial solution, it is advantageous to introduce a compact notation. Let $\bar{\mathbf{F}}$ be a column vector with the $g \times (2L+1)$ unknown variables $F_{M_i}^{L\pi S}$ arranged in the following order:

$$\bar{\mathbf{F}} = \begin{pmatrix} \bar{F}_{-L} \\ \bar{F}_{-L+1} \\ \vdots \\ \bar{F}_L \end{pmatrix}, \quad (28)$$

where

$$\bar{F}_{M_i} = \begin{pmatrix} F_{M_i^1} \\ F_{M_i^2} \\ \vdots \\ F_{M_i^g} \end{pmatrix}, \quad (29)$$

with the subscripts L , π and S left out. The general solution to the problem can then be written

$$\begin{pmatrix} \mathcal{K}(X^1, Y^1) - I_{g(2L+1)} \\ \vdots \\ \mathcal{K}(X^q, Y^q) - I_{g(2L+1)} \end{pmatrix} \bar{\mathbf{F}} = 0, \quad (30)$$

where the Kronecker tensor product, $\mathcal{K}(X, Y)$, of two matrices, X and Y , is a larger matrix formed by taking all possible products between the elements of X and those of Y . If X is an $m \times n$ matrix ($X \in \mathcal{M}_{m,n}$) and $Y \in \mathcal{M}_{p,q}$ then $\mathcal{K}(X, Y) \in \mathcal{M}_{mp, nq}$, and the elements are arranged in the following order:

$$\mathcal{K}(X, Y) = \begin{pmatrix} X_{11}Y & X_{12}Y & \dots & X_{1n}Y \\ X_{21}Y & X_{22}Y & & \\ \vdots & & \ddots & \\ X_{m1}Y & & & X_{mn}Y \end{pmatrix}. \quad (31)$$

Furthermore, in Eq. (30), q denotes the number of symmetry operations, $X \in \mathcal{M}_{2L+1}$, $Y \in \mathcal{M}_g$, and I_m is a $m \times m$ identity matrix. Table I lists the matrix elements of X and Y for each system. A given term ${}^{2S+1}L^\pi$ is accessible for the energy-favorable arrangement if and only if Eq. (30) has a nontrivial solution.

TABLE II. Classification scheme for two-valence-electron atoms with $L \leq 4$, especially valid for doubly excited intra-shell states. For a given L , terms which are line accessible are expected to have lower energy than line-inaccessible terms.

	Line-accessible terms	Line-inaccessible terms
$L=0$	$1S^e$	$1S^o, 3S^o, 3S^e$
$L=1$	$3P^o$	$1P^o, 1P^e, 3P^e$
$L=2$	$1D^e, 3D^o$	$1D^o, 3D^e$
$L=3$	$1F^e, 3F^o$	$1F^o, 3F^e$
$L=4$	$1G^e, 3G^o$	$1G^o, 3G^e$

V. RESULTS

A. Two-electron systems

Table II displays the classification of two-valence-electron atoms. We note that the only line-accessible S state is $1S^e$.

B. Three-electron systems

The classification of the three-electron system is given in Table III. It is useful to compare the classification of the states in the table with Fig. 3 which shows all $3I3I'3I''$ triply excited states in the lithiumlike ion He^- with $L \leq 4$ ordered along each column according to $^{2S+1}L^\pi$ symmetry. The energies were calculated within a model with frozen radial degrees of freedom [16]. The model was quantitatively justified by multiconfigurational Hartree-Fock calculations [28] and by calculations with the hyperspherical method [29]. The ET-accessible states are marked by dashed lines in Fig. 3. We see from the figure that no ET-accessible S states exist (see also Table III). For all other L values considered, the lowest-lying state is ET accessible. Furthermore, the energy of the lowest state of a specific symmetry is lower for small L . This energy behavior is qualitatively explained by comparison with the rotational part of the energy spectrum for a symmetric top molecule [$\propto L(L+1)$] [16]. The S states do not follow this trend in agreement with the fact that they are ET inaccessible.

C. Four-electron systems

RTH-accessible states listed in Table IV are in agreement with the classification in Refs. [20,26]. In these works the

TABLE III. Classification scheme for three-valence-electron atoms with $L \leq 4$, especially valid for triply excited intra-shell states. For a given L , equilateral triangle (ET) accessible terms are expected to have lower energy than ET inaccessible terms.

	ET accessible terms	ET inaccessible terms
$L=0$		$2S^o, 2S^e, 4S^o, 4S^e$
$L=1$	$2P^o, 4P^e$	$2P^e, 4P^o$
$L=2$	$2D^o, 2D^e$	$4D^o, 4D^e$
$L=3$	$2F^o, 2F^e, 4F^o, 4F^e$	
$L=4$	$2G^o, 2G^e, 4G^o$	$4G^e$

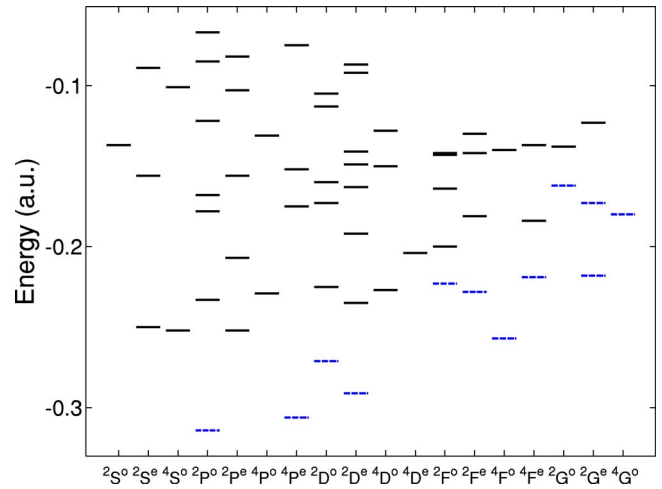


FIG. 3. (Color online) Energy levels of $3I3I'3I''$ triply excited states in He^- with $L \leq 4$ calculated within the frozen- r model [16]. The states are ordered according to $^{2S+1}L^\pi$ symmetry, and equilateral triangle (ET)-accessible states are marked by dashed lines.

classification was performed with respect to a different body-fixed frame. The identity of the results reflects that overall rotations with respect to a fixed laboratory system are unimportant. From Table IV, it is seen that the $5S^o$ state is RTH accessible. This is in agreement with the multiconfigurational Hartree-Fock calculation predictions of Ref. [30] where it was concluded that the inter-electronic angle in the $5S^o$ state tends to be that of tetrahedral geometry ($109,5^\circ$) when the excitation n grows. This result also shows that the classification is particularly valid for quadruply excited intrashell states. Energies of quadruply excited intra-shell RTH-accessible states were recently calculated within an analytical model [22]. The model was inspired by the spatial arrangement of Fig. 1(c), and was quantitatively justified by comparison with multiconfigurational Hartree-Dirac-Fock calculations.

D. Six-electron systems

The classification in Table V distinguishes terms with $L \leq 4$ which are ROH-accessible and which consequently are expected to belong to the lowest-lying part of the energy spectrum from ROH-inaccessible terms.

TABLE IV. Classification scheme for four-valence-electron atoms with $L \leq 4$, especially valid for quadruply excited intra-shell states. For a given L , RTH-accessible terms are expected to have lower energy than RTH-inaccessible terms.

	RTH-accessible terms	RTH-inaccessible terms
$L=0$	$5S^o$	$1S^o, 1S^e, 3S^o, 3S^e, 5S^e$
$L=1$	$3P^e$	$1P^o, 1P^e, 3P^o, 5P^o, 5P^e$
$L=2$	$1D^o, 1D^e, 3D^o$	$3D^e, 5D^o, 5D^e$
$L=3$	$3F^o, 3F^e, 5F^e$	$1F^o, 1F^e, 5F^o$
$L=4$	$1G^o, 1G^e, 3G^o, 3G^e, 5G^o$	$5G^e$

TABLE V. Classification scheme for six-valence-electron atoms with $L \leq 4$, especially valid for sextuple excited intra-shell states. For a given L , ROH-accessible terms are expected to have lower energy than ROH-inaccessible terms.

	ROH-accessible terms	ROH-inaccessible terms
$L=0$	$1S^o, 1S^e$	$3S^o, 3S^e, 5S^o, 5S^e, 7S^o, 7S^e$
$L=1$	$3P^o, 3P^e$	$1P^o, 1P^e, 5P^o, 5P^e, 7P^o, 7P^e$
$L=2$	$1D^e, 3D^o, 5D^o, 5D^e$	$1D^o, 3D^e, 7D^o, 7D^e$
$L=3$	$1F^e, 3F^o, 3F^e, 5F^e, 7F^o$	$1F^o, 5F^o, 7F^e$
$L=4$	$1G^o, 1G^e, 3G^o, 3G^e, 5G^o, 5G^e$	$7G^o, 7G^e$

VI. CONCLUSION

In conclusion, we discuss a method to classify atomic states independent of the model describing the dynamics of the system. The assumption in the model is that the system prefers the geometry which minimizes the potential energy. It may happen, however, that inherent nodal surfaces arising from quantum-mechanical symmetry constraints impose restrictions on this preferred geometric configuration. Thus the relative energies among states of different symmetry are on one hand determined by geometrical symmetry and on the other hand constrained set by quantum-mechanical symmetry. A comparison of the classification scheme and the spectrum of the $3I3I'3I''$ states in He^- confirmed the expectations derived from the model. The present classifications are expected to be useful for the study of multiply excited states.

ACKNOWLEDGMENTS

We thank J. Linderberg, J. Olsen and C. Zickert for useful discussions. L.B.M. is supported by the Danish Natural Science Research Council (Grant No. 21-03-0163).

APPENDIX A: REPRESENTATION THEORY OF THE PERMUTATION GROUP

In this Appendix some results of the Young-Yamanouchi theory are summarized. The content is based on Refs. [31–33].

The connection between a system of n identical fermions and the permutation group, S_n , is that the Pauli principle requires the system to have permutation symmetry. An anti-symmetrized eigenstate of identical fermions can be expanded in the so-called Young-Yamanouchi basis as

$$|\Psi^{LM\pi, SM_S}\rangle = \sum_i F_{M,i}^{L\pi S} \chi_{M_S,i}^S, \quad (\text{A1})$$

where the summation is over all possible couplings of intermediate spin. In this expression each spin function $\chi_{M_S,i}^S$ belongs to a particular Young tableau and the spatial function $F_{M,i}^{L\pi S}$ that multiplies this particular spin function belongs to the conjugate tableau (see below.)

Let us consider the permutation group S_n . A *partition* is the splitting-up of the integer n into a sum of integers, λ_i , satisfying

$$\lambda_1 + \lambda_2 + \dots + \lambda_h = n, \quad \lambda_1 \geq \lambda_2 \geq \dots \geq \lambda_h. \quad (\text{A2})$$

The partitions of $n=4$, e.g., are $[4], [3,1], [2,2] \equiv [2^2], [2,1,1] \equiv [2,1^2]$ and $[1,1,1,1] \equiv [1^4]$. A partition can be pictured as a *Young diagram* which is an arrangement of n cells in h rows; each row begins with the same vertical line and the number of cells in successive rows are $\lambda_1 \geq \lambda_2 \geq \dots \geq \lambda_h$. The Young diagrams for $n=4$ are

$$[4] \begin{array}{|c|c|c|c|} \hline \square & \square & \square & \square \\ \hline \end{array} \quad [3,1] \begin{array}{|c|c|c|} \hline \square & \square & \square \\ \hline \square & & \\ \hline \end{array} \quad [2,2] \begin{array}{|c|c|} \hline \square & \square \\ \hline \square & \square \\ \hline \end{array} \quad [2,1^2] \begin{array}{|c|c|} \hline \square & \square \\ \hline \square & \square \\ \hline \square & \\ \hline \end{array} \quad [1^4] \begin{array}{|c|} \hline \square \\ \hline \square \\ \hline \square \\ \hline \square \\ \hline \end{array}. \quad (\text{A3})$$

Two Young diagrams are said to be *conjugate* if they are obtained from each other by an interchange of rows and columns.

There is a one to one correspondence between the inequivalent irreducible representations of S_n and the partitions. In addition, the dimension of an irreducible representation is equal to the number of *Young tableaux* that can be constructed from the corresponding partition. A Young tableau is a Young diagram with the numbers $j=1, 2, \dots, n$ arranged in the cells such that the numbers increase as one moves to the right and one goes down. The Young tableaux for the partition $[31]$ are

$$[31] \begin{array}{|c|c|c|} \hline 123 & 124 & 134 \\ \hline 4 & 3 & 2 \\ \hline \end{array} \quad (\text{A4})$$

The Young tableaux give the *Young-Yamanouchi basis vectors*, $Y_i^{[\lambda]}$. In Eq. (A1) it is understood that the Young-Yamanouchi basis vector belonging to the spin state is multiplied by a basis vector belonging to the conjugate tableau for the spatial wave function.

An irreducible representation of S_n represented by a partition $[\lambda]$ is reducible with respect to its subgroup $S_{n-1} \subset S_n$. This implies that the representatives, $G^{[\lambda]}(\mathbf{P})$, of elements \mathbf{P} belonging to the subgroup S_{n-1} are on block-diagonal form

$$G^{[\lambda_1 \dots \lambda_j \dots \lambda_h]}(\mathbf{P}) = \sum_{j=h}^1 \oplus G^{[\lambda_1 \dots \lambda_{j-1} \dots \lambda_h]}(\mathbf{P}), \quad \mathbf{P} \in S_{n-1}, \quad (\text{A5})$$

where the summation is restricted to partitions, which means $\lambda_j - 1 \geq \lambda_{j+1}$. As an example, we consider the partition $[42]$ of S_6

$$G^{[42]}(\mathbf{P}) = \left(\begin{array}{c|c} G^{[41]}(\mathbf{P}) & \\ \hline & G^{[32]}(\mathbf{P}) \end{array} \right), \quad \mathbf{P} \in S_5. \quad (\text{A6})$$

The irreducible matrices of all elements of S_n can be found once those of the generators $\mathbf{P}_{n-1,n} = (n-1, n)$, for S_n, S_{n-1}, \dots, S_1 are known. This follows from Eq. (A5) and the following two identities for permutations:

$$(j, j + \nu) = (j + 1, j + \nu)(j, j + 1)(j + 1, j + \nu), \quad (\text{A7})$$

$$(\alpha\beta\gamma\delta) = (\alpha\beta)(\beta\gamma)(\gamma\delta). \quad (\text{A8})$$

Now, to find the irreducible matrices of the generators $\mathbf{P}_{n-1,n} = (n-1, n)$ of S_n , i.e., to find $G_{ii}^{[\lambda]}(j, j+1) = \langle Y_i^{[\lambda]} | (j, j$

$+1)|Y_{i'}^{[\lambda]} \rangle, j=1, \dots, n-1$ we use the following simple rules: Consider the Young-Yamanouchi basis vectors $Y_i^{[\lambda]}$ and find the numbers j and $j+1$ in the corresponding Young tableau.

(1) If j and $j+1$ are in the same column/row of the Young tableau $Y_i^{[\lambda]}$ then

$$G_{ii'}^{[\lambda]}(j, j+1) = \pm 1 \quad (\text{A9})$$

(2) If j and $j+1$ are neither in the same column nor the same row of the Young tableau $Y_i^{[\lambda]}$ then

$$G_{ii'}^{[\lambda]}(j, j+1) = \begin{cases} 1/\sigma, & i' = i \\ -\sqrt{\sigma^2 - 1}/|\sigma|, & \text{when } Y_{i'}^{[\lambda]} = (j, j' + 1)Y_i^{[\lambda]} \\ 0 & \text{otherwise,} \end{cases} \quad (\text{A10})$$

where σ is the axial distance given by

$$\sigma = r_{j+1} - r_j - (c_{j+1} - c_j), \quad (\text{A11})$$

with $r_j, r_{j+1}(c_j, c_{j+1})$ being row (column) numbers of j and $j+1$ in the Young tableau $Y_i^{[\lambda]}$

Our phase convention follows Ref. [32].

Let us consider, as an example, the case of four electrons with total spin $S=1$. First we identify a partition corresponding to $S=1$. This can be done with the formula

$$S = \frac{1}{2}(\lambda_1 - \lambda_2), \quad (\text{A12})$$

with $\lambda_1 + \lambda_2$ equal to the number of electrons. We see that $\lambda_1=3$ and $\lambda_2=1$ corresponding to the partition $[31]$ fulfills this requirement as well as (A12). To find $G^{[31]}(P_{34})=G^{[31]} \times (34)$ we consider the Young tableaux in Eq. (A4) and use Eqs. (A9) and (A10)

$$G_{11}^{[31]}(34) = \left\langle \begin{array}{c} 123 \\ 4 \end{array} \middle| (34) \begin{array}{c} 123 \\ 4 \end{array} \right\rangle = \frac{1}{3}, \quad (\text{A13})$$

$$G_{12}^{[31]}(34) = \left\langle \begin{array}{c} 123 \\ 4 \end{array} \middle| (34) \begin{array}{c} 124 \\ 3 \end{array} \right\rangle = -\frac{\sqrt{8}}{3}, \quad (\text{A14})$$

$$G_{13}^{[31]}(34) = \left\langle \begin{array}{c} 123 \\ 4 \end{array} \middle| (34) \begin{array}{c} 134 \\ 2 \end{array} \right\rangle = 0, \quad (\text{A15})$$

$$G_{22}^{[31]}(34) = \left\langle \begin{array}{c} 124 \\ 3 \end{array} \middle| (34) \begin{array}{c} 124 \\ 3 \end{array} \right\rangle = -\frac{1}{3}, \quad (\text{A16})$$

$$G_{23}^{[31]}(34) = \left\langle \begin{array}{c} 124 \\ 3 \end{array} \middle| (34) \begin{array}{c} 134 \\ 2 \end{array} \right\rangle = 0, \quad (\text{A17})$$

$$G_{33}^{[31]}(34) = \left\langle \begin{array}{c} 134 \\ 2 \end{array} \middle| (34) \begin{array}{c} 134 \\ 2 \end{array} \right\rangle = -1. \quad (\text{A18})$$

Since the Yamanouchi matrices are symmetric, it suffices to determine the elements of their upper triangular parts.

-
- [1] N. Bohr, *Philos. Mag.* **26**, 1 (1913).
 - [2] J. W. Nicholson, *Mon. Not. R. Astron. Soc.* **72**, 49 (1911).
 - [3] W. Heisenberg, *Z. Phys.* **33**, 879 (1925).
 - [4] E. Schrödinger, *Ann. Phys.* **79**, 361 (1926).
 - [5] D. R. Hartree, *Proc. Cambridge Philos. Soc.* **26**, 89 (1928).
 - [6] V. Fock, *Z. Phys.* **61**, 126 (1930).
 - [7] G. H. Wannier, *Phys. Rev.* **90**, 817 (1953).
 - [8] H. Klar and W. Schlecht, *J. Phys. B* **10**, 1699 (1976).
 - [9] P. Grujić, *Phys. Lett.* **96**, 233 (1983).
 - [10] P. Grujić, *Phys. Lett. A* **122**, 494 (1987).
 - [11] M. Y. Kuchiev and V. N. Ostrovsky, *Phys. Rev. A* **58**, 321 (1998).
 - [12] V. N. Ostrovsky, *Phys. Rev. A* **64**, 022715 (2001).
 - [13] G. F. Gribakin, S. Sahoo, and V. N. Ostrovsky, *Phys. Rev. A* **70**, 062717 (2004).
 - [14] C. D. Lin, *Phys. Rev. A* **29**, 1019 (1984).
 - [15] C. D. Lin, *Adv. At. Mol. Phys.* **22**, 77 (1986).
 - [16] T. Morishita and C. D. Lin, *Phys. Rev. A* **64**, 052502 (2001).
 - [17] L. B. Madsen and K. Mølmer, *Phys. Rev. Lett.* **87**, 133002 (2001).
 - [18] L. B. Madsen, *J. Phys. B* **36**, R223 (2003).
 - [19] Chen Guang Bao, *Phys. Rev. A* **47**, 1752 (1993).
 - [20] C. G. Bao, *Commun. Theor. Phys.* **29**, 491 (1996).
 - [21] C. G. Bao and Y. X. Liu, *Phys. Rev. Lett.* **82**, 61 (1999).
 - [22] M. D. Poulsen and L. B. Madsen, *Phys. Rev. A* **71**, 062502 (2005).
 - [23] C. G. Bao, W. F. Xie, and C. D. Lin, *J. Phys. B* **27**, L193 (1994).
 - [24] Chen Guang Bao, *Phys. Rev. A* **50**, 2182 (1994).
 - [25] C. G. Bao, X. Yang, and C. D. Lin, *Phys. Rev. A* **55**, 4168 (1997).
 - [26] C. G. Bao, *Phys. Lett. A* **250**, 123 (1998).
 - [27] R. N. Zare, *Angular Momentum* (Wiley and Sons, New York, 1988).
 - [28] Y. Komninos, M. Chrysos, and C. A. Nicolaides, *Phys. Rev. A* **38**, 3182 (1988).
 - [29] T. Morishita and C. D. Lin, *Phys. Rev. A* **59**, 1835 (1999).
 - [30] Y. Komninos and C. A. Nicolaides, *Phys. Rev. A* **50**, 3782 (1994).
 - [31] M. Weissbluth, *Atoms and Molecules* (Academic Press, San Diego, 1978).
 - [32] M. Kotani, A. Amemiya, E. Ishiguro, and T. Kimura, *Tables of Molecular Integrals* (MARUZEN Co. Ltd., Tokyo, 1963).
 - [33] J. Q. Chen, J. Ping, and F. Wang, *Group Representation Theory for Physicists* (World Scientific, Singapore, 1989).